J. Mt. Sci. (2014) 11(4): 825-837 e-mail: jms@imde.ac.cn http://jms.imde.ac.cn
DOI: 10.1007/s11629-014-2985-5

An Artificial Neural Network-Based Snow Cover Predictive Modeling in the Higher Himalayas

Bhogendra MISHRA[1]*, Nitin K. TRIPATHI[1], Mukand S. BABEL[2]

1 Remote Sensing and Geographical Information Systems, Asian Institute of Technology, P.O. Box 4, Klong Luang, Pathumthani 12120, Thailand

2 Water Engineering and Management, Asian Institute of Technology, P.O. Box 4, Klong Luang, Pathumthani 12120, Thailand

**Corresponding author, e-mail: bhogendra@gmail.com*

Citation: Mishra B, Tripathi NK, Babel MS, et al. (2014) An artificial neural network-based snow cover predictive modeling in the higher Himalayas. Journal of Mountain Science 11(4). DOI: 10.1007/s11629-014-2985-5

Abstract: With trends indicating increase in temperature and decrease in winter precipitation, a significant negative trend in snow-covered areas has been identified in the last decade in the Himalayas. This requires a quantitative analysis of the snow cover in the higher Himalayas. In this study, a nonlinear autoregressive exogenous model, an artificial neural network (ANN), was deployed to predict the snow cover in the Kaligandaki river basin for the next 30 years. Observed climatic data, and snow covered area was used to train and test the model that captures the gross features of snow under the current climate scenario. The range of the likely effects of climate change on seasonal snow was assessed in the Himalayas using downscaled temperature and precipitation change projection from - HadCM3, a global circulation model to project future climate scenario, under the A1B emission scenario, which describes a future world of very rapid economic growth with balance use between fossil and non-fossil energy sources. The results show that there is a reduction of 9% to 46% of snow cover in different elevation zones during the considered time period, i.e., 2011 to 2040. The 4700 m to 5200 m elevation zone is the most affected area and the area higher than 5200 m is the least affected. Overall, however, it is clear from the analysis that seasonal snow in the Kaligandaki basin is likely to be subject to substantial changes due to the impact of climate change.

Keywords: Snow cover; Kaligandai river; Himalayas; Artificial neural network; Global warming; Climate change

Received: 10 January 2014
Accepted: 16 April 2014

Introduction

Global warming will impact the extent, amount and duration of snow cover in the Himalayas. The results of many studies have shown a significant decline in snow cover due to warming in the last couple of decades (Kulkarni et al. 2007; Li et al. 2012) and this declining trend is likely to continue in the future. This prediction is based on the forecast of climate variables in several parts of the world. However, the predicted change is not consistent (as far as the intensity of the change is concerned) in all of these studies (Bolch et al. 2012; Mallapaty 2014). Many previous studies are likely to have over-estimated the resulting impact of climate change (Bolch et al. 2012; Cooke 2014; Karmacharya et al. 2007; Xu et al. 2009).

Snowmelt is a complex phenomenon which does not depend exclusively on climatic factors alone. Several researchers have found that environmental and microbiological factors such as

dust deposition, primary colonization, degradation of dust biomass, deposition of potentially pathogenic microbial species and resulting increased leaching of minerals can also contribute to the process of snowmelt (Chatterjee et al. 2010; Decesari et al. 2009; Stres et al. 2010; Stres et al. 2013). Combining topographic, climatic, environmental and microbiological factors towards snowmelt may be a complex model. However, the autoregressive neural network is envisaged to capture this complex phenomenon as the data input and output are taken based on remote sensing imageries.

A new way of prediction that uses artificial neural network (ANN) has become more popular in the last few years compared to the traditional prediction techniques like regression analysis, time series analysis etc. in several sectors such as flood forecasting, water demand forecasting, un-gauged stream flow forecasting etc.. (Babel and Shinde 2010; Besaw et al. 2010; Chen et al. 2010). The ANN models are gaining popularity for several hydrological phenomena predictions, because these models are able to map the nonlinear trend of several phenomena simultaneously. One study carried out by Jain et al. (2001) shows that ANN can perform better than the existing regression and time series analysis of water demand forecasting. In recent studies carried out by Besaw et al. (2010) and Chen et al. (2010), researchers could forecast the un-gauged stream flow and flood, and concluded that ANN outperformed the existing time series modeling techniques and regression models. Several other researchers have also accepted the usability of ANN in time series forecasting (Maier et al. 2010; Besaw et al. 2010, among others).

A nonlinear autoregressive exogenous model (NARX) was evaluated and verified with several chaotic time series data with differing- different configurations. The NARX model is recommended for dynamic system application (Diaconescu, 2008). Several long term snow cover trends have been published, with a focus on Central Europe and New Zealand (Hantel and Hirtlewielke 2007; Hendrikx and Hreinsoon 2012). The main focus of such studies was snow cover variability in the context of global warming, and the variability's influence on ski tourism in New Zeland and Central Europe. Another study in Central Europe was attempted to predict the snow cover in the Black Forest mountain range using NARX with remote sensing and Geographical Information Systems (GIS). The researchers of this study used the Levenberg-Marquad algorithm to optimize the network (Sauter et al. 2010). The study conducted by Shen and Chang (2013) used NARX to forecast multistep-ahead inundation depth in an inundation area and gave the better result than feedforward time-delay and an online feedback configuration of NARX networks. Similarly, NARX gave a superior result on downscaling of meteorological fields meso-scale water balance modeling in comparison to the coupling between recurrent neural network and a distributed water shed model (Kronenberg et al. 2013).

Another work (Quiroga et al. 2013) used ANN and multiple linear regression models (MLR) to estimate the melting of snow and glaciers and found that ANN models outperformed the MLR models at the Condoriri Glacier in Bolivia. Chen and Chang (2009) used the revolutionary ANN for hydrological system forecasting. The genetic algorithm and scaled conjugate gradient algorithm were used to optimize the feed forward algorithm. The results were compared with AR and ARMAX methods.

Several models and techniques for climate change modeling and future prediction are available. The ANN is one of them. Forecasting of water resource variables using ANN has developed as a reliable tool in the last few decades (Nourani et al. 2012). However, even the finest network architecture and characteristics of neural networks are absolutely problem dependent and there is no established methodology available to deal with water resources and the modeling problems of climate change impact. Some sort of preliminary forecast analysis can be performed for a particular location based on the time series analysis using different architectures and properties of the network (Babel and Shinde 2010). Some of the commonly used networks in this field are the feed forward neural network, the multilayer feed forward neural network, the partially recurrent neural network, and the time delay neural network etc. (Besaw et al. 2010; Babel and Shinde 2010; Chen et al. 2010). In these networks, several kinds of transfer functions, like log sigmoid, hard limit etc. can be implemented (Maier et al. 2010; Jain et

al. 2001).

A large amount of research activities using ANN has led to a number of publications that conform the potential of ANN for the prediction and forecasting of water resource variables. However, several challenges are still to be overcome before it becomes a reliable modeling approach. The difficulties include the unavailability of optimal network architecture because the properties of neural networks are highly problem-dependent. In his review, Welsh (2008) suggested that attention to the development of a good model is vital.

The prediction accuracy of ANN relies greatly on the input variables, which are influential parameters. It is widely accepted that snow covered area is governed by various climatic and topographic parameters (Dery et al. 2005). These parameters may vary from place to place; thus, it is necessary to develop site or region specific models for snow cover area forecasting.

The use of ANN for snow cover area forecasting is relatively new but it has already proven its ability in several other hydrological phenomena's predictions.

The main aim of this study is to explore the uses of ANN for long term snow cover forecasting using the given climate variables. A selected ANN model was trained using selected observed, and remote sensing climatic variables and the corresponding snow covered area was used as output. In addition, the climatic variables obtained from the selected scenario of the General Circulation Model (GCM) were used as input variables and the corresponding snow cover area was predicted.

1 Study Area

The study area is located in the central part of northern Nepal. It covers the area between 27°56'40"N to 29°19'22"N and 82°54'57"E to 85°06'30"E. The area includes the Kaligandaki basin, one of the major tributaries of the Gandaki River (Figure 1). The minimum temperature in the higher mountainous region drops to -25°C or even less in winter, and the maximum temperature in the lower part of the study area reaches up to 35°C or above in summer (Mishra et al. 2014). Precipitation distribution also varies greatly with respect to spatial location and time of the year. Though precipitation is dominant during the monsoons in summer, maximum snowfall occurs due to the westerly winds in winter. During the summer season (June - August), the monsoons produce heavy precipitation that contributes approximately 80% of the annual precipitation. Precipitation intensity goes down from east to west and south to north. In the western Himalayas, westerly winds cause winter (December - February) precipitation, mostly in the form of snow (Rees and Collins 2006). Other seasons, namely autumn (September - November) and spring (March - May), witness occasional rainfall that contributes about

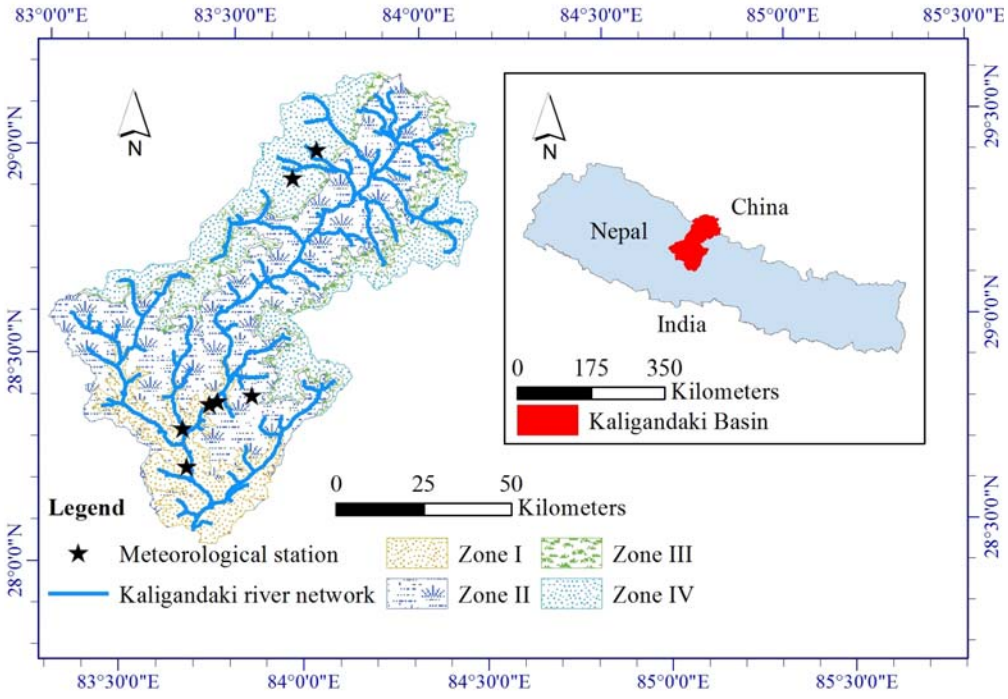

Figure 1 Study area, Kaligandaki river basin, Nepal.

15% to the annual rainfall. In spring, precipitation is in the form of rainstorms and snowstorms. In summer, the maximum snowmelt runoff occurs and hence the snow covered area becomes minimal (Mishra et al. 2014).

Land use greatly depends on altitude. As per the map developed from the MODIS image, approximately 24% of the Kaligandaki basin area is under perennial snow cover, 20% is under seasonal snow cover, 27% is covered by forests and shrubs, 11% is used for village settlements and agricultural lands, and 18% for rivers and grazing fields.

The altitude of the basin varies from 590 to 8148 m a.s.l.. The upper parts, in general, have higher slopes compared to the lower parts of the basin. The hypsometric analysis of the basin depicts that about 1638 km² (24.43% of the total basin area) is located on altitudes higher than 5200 m a.s.l.. It also shows that the Kaligandaki basin is uniformly distributed with respect to elevation, with a nearly linear line except at higher elevations with a very steep slope, as shown in Figure 2.

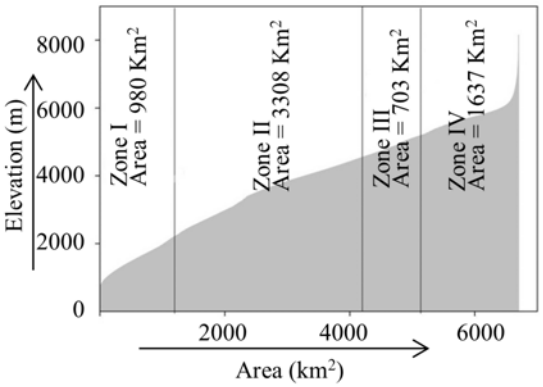

Figure 2 Study area – hypsometric elevation and zoning, the zoning was done based on snow cover timing, zone I – snow free area, zone II – occasional snow cover or snow cover in winter, zone III – snow cover all over the year except in summer, and zone IV – perennial snow cover area.

In our previous work (Mishra et al. 2014), the Kaligandaki river basin was divided into four zones for the study's purpose. As this is a continuation of the same line of work, we have used the same division here as well. Zone I covers the area between 590 and 2000 m a.s.l. with no snow cover. Since Zone I is almost snow free all through the year, we did not consider this zone for the task of forecasting. Zone II covers the area from 2000 to 4700 m a.s.l., and is influenced by a seasonal snow cover. The lower part of this zone is covered by snow only in the winter season whereas the upper part is covered by snow during three seasons — winter, early spring and autumn — and is covered by green vegetation in late spring and summer. The basin area from 4700 to 5200 m a.s.l. is included in Zone III, which is completely snow covered except for one or two months in summer and very rarely can vegetation be seen even during this period because of extreme cold conditions. The area above the elevation of 5200 m a.s.l. is considered to be under Zone IV, and this zone is permanently covered by snow.

2 Data Used

Remote sensing was the main source of data in this study. Various products from several sensors such as a precipitation derived from Tropical Rainfall Measuring Mission (TRMM): 3B43 (Huffman et al. 2007), a Moderate Resolution Imaging Spectro-Radiometer (MODIS) snow propduct MOD10A2, MODIS temperature MOD11C3 (Riggs et al. 2006), etc. were employed. The images were re-projected into the UTM 45 North with World Geodetic System 1984 (WGS84) datum as per requirement. This data was obtained from several online data sources for the period of 2000 to 2010. These are described below.

2.1 MODIS snow cover mapping

The MODIS has provided a large number of snow products. MOD10A2, MODIS/Terra snow cover 8-day L3 Global 500 m spatial resolution product, has been used in this study (Hall et al. 2006). The key for snow detection characteristics is to have a high reflectance in the visible bands (0.40 to 0.70 μm) and very low reflectance in near-infrared bands (1.628 to 1.652 μm) (Riggs et al. 2006). Band 4 (green 0.545 to 0.565 μm) and Band 6 (near-infrared 1.628 to 1.652 μm) were used to derive snow cover products from MODIS images. By using these two bands, the Normalized Difference Snow Index (NDSI) was obtained using the following relation (Riggs et al. 2006):

$$NDSI = \frac{band\ 4 - band\ 6}{band\ 4 + band\ 6} \quad (1)$$

In non-forested areas, a pixel with an NDSI ≥ 0.4 was identified as snow covered if the reflectance in Band 2 (0.841 - 0.876 μm) is ≥11% and the reflectance in Band 4 (0.545 -0.565 μm) is ≥ 10% (Hall et al. 1995). In a forested area, an alternative algorithm is used that includes the Normalized Difference Vegetation Index (NDVI). For a forested area, the threshold value of NDVI can be used to classify the pixel as snow even if the NDSI is lower than 0.4 (Klein et al. 1998). This product was validated in several places in the Himalayas, including the Kaligandaki basin (Mishra et al. 2014). The snow product generated from high resolution Advanced Spaceborne Thermal Emission Reflection Radiometer (ASTER) image was used to validate the MOD10A2 product in the Kaligandaki basin. MODIS snow product can be downloaded freely from the National Snow and Ice Data Center (http://nsidc.org/data/mod10a2).

2.2 MODIS temperature

MODIS land surface product, MOD11C3, is the monthly product of MODIS/TERRA with 0.05° of spatial resolution and provides per pixel temperature. This land surface temperature product has already been validated for ground air temperature in several parts of the world, including in the Himalayas (Maskey et al. 2011; Wang et al. 2007; Wang et al. 2008). MOD11C3 was used for the model training and testing. This product is available in Land Processes Distributed Active Archive Center (LP DAAC).

2.3 TRMM precipitation

A 3B43 product was selected for this study. This monthly product covers the area of 50° N to 50°S with a spatial resolution of 0.25°. This product was developed in three steps: first, several passive microwave sensors on the board of the TRMM and other satellites were converted to a precipitation estimate. In the next step, an infrared (IR) estimate using the calibrated microwave estimate was made. As a third step, the microwave and the IR estimates were combined to provide the best estimation of precipitation. The final step while generating 3B43 was the inclusion of rain gauge data. The three hourly estimates obtained by combining microwaves and IR estimates were then summed up over a calendar month to create a monthly multi-satellite product (Huffman et al. 2007). This product is freely available at http://disc.sci.gsfc.nasa.gov/precipitation/documentation/TRMM_README/TRMM_3B43_readme.shtml.

2.4 GCM selection

A general circulation model (GCM) is a mathematical model used to simulate the earth atmosphere. It may work differently for the oceans and the atmosphere or in a tightly coupled manner. GCMs are widely used for forecasting climate variability as well as for projecting climate changes. Several GCMs are available based on different mathematical modeling techniques and they forecast differently. These differences regarding forecasting are called the element of uncertainty. It is important to consider topography, environment, etc. in order to select an appropriate GCM having a small amount of uncertainty.

Many GCMs project global climatic variables under different scenarios, but their resolution, representativeness of the study domain and availability of data to the public makes it difficult to select the most appropriate GCM. In this study, all future climatic changes are based on the HadCM3 model, a coupled atmosphere-ocean general circulation model developed at the Hadley Centre in the United Kingdom (Pope et al. 2000). It is the successor to HadCM2 used in IPCC third assessment report and has the resolution of 2.5 × 3.75 (Khadka et al. 2014). The A1B emission scenario, is a group under A1 family which describes a future world of very rapid economic growth, global population that peaks in mid-century and declines thereafter, and the rapid introduction of new and more efficient technologies. A1B signifies balance use between fossil and white energy sources (Khadka et al. 2014). Under this scenario, the average linear air temperature trend is of about 0.26°-0.28°C per decade. This is very close to the increasing temperature trend obtained since 1980 in the Kaligandaki basin in our previous study (Mishra et al. 2014). Thus, based on this accuracy, the HadCM3 model with the A1B scenario was chosen in the analysis. Additionally, A1B is a moderate global warming scenario, and lies between two

extreme scenarios i.e. little warming and strong warming (IPCC 2007). Thus, A1B is more likely to represent the real situation for the future than an extreme scenario.

3 Methodology

3.1 Selection of input variables

The accuracy of the prediction depends greatly upon the explanatory variables employed as influential parameters (Babel and Shinde 2010). It is widely accepted that the snow cover area is determined by various climatic and topographic factors which differ from place to place, thus necessitating the need to find a site/region specific input parameters. In addition, to reduce the complexity of the model, only very precise input variables must be used (Noori et al. 2010). The most commonly used measure of statistical dependency for input selection is correlation coefficient (Maier et al. 2010), therefore, it has been used to find the dependency and discard the dependent climatic variable while selecting the input set in this study and calculated using Equation 2.

$$r = \frac{n\sum xy - \sum x \sum y}{\sqrt{n\sum x^2 - \left(\sum x\right)^2}\sqrt{n\sum y^2 - \left(\sum y\right)^2}} \quad (2)$$

where x, y are two variables subjected to calculate the correlation coefficient and n is the number of population.

The value of r can be in between -1 and +1, with -1 perfect negative relationship, +1 is perfect positive relationship and 0 is no relationship between x and y. Thus, the closer r is to -1 the stronger the negative linear relationship and the closer r is to 1, the stronger the positive linear relationship.

3.2 Non-linear autoregressive networks with an exogenous network

ANN attempts to simulate the workings of the neurons in the brain by using a network of artificial neurons organized in layers, which receive a stimulus and, via a transfer function, mathematically convert the said stimulus into an output signal. If the selected process is deterministic and linear, the implementation will be straightforward. However, the accumulation and melting processes of snow are highly non-linear and vary both spatially and temporally. There is usually a strong dependence on initial conditions and small fluctuations in the independent variables, which can cause great variations in the response system. The system can be heavily influenced by external input climate variables that are dynamic in nature. Besides, it is common that datasets are not noise-free because of several reasons like measurement error, processing errors etc. Such complex time-series data require a stable model that can cope with a non-linear environment and can produce long term dynamics in a statistical sense rather than focus on short term predictions. To guarantee a considerably accurate forecasting, the model must yield the time series snow cover area with the same statistical properties as the original data. In order to ensure these requirements, NARX was chosen to forecast the snow cover area in this study. NARX belongs to the class of recurrent dynamic networks with feed back connections. It is based on the linear autoregressive exogenous (ARX) model which is commonly used in the time series modelling (Connor and Martin 1994). Equation 3 represents the NARX model.

$$\begin{aligned} y(t) = f(&y(t-1), y(t-2).....y(t-q), \\ &\varphi(t-1), \varphi(t-2).....\varphi(t-q)) \end{aligned} \quad (3)$$

where $y(t)$ is the model output regressed on previous values $y(t\text{-}1)$ with a delay of q time steps as well as further exogenous parameters φ. The function f is an unknown non-linear mapping function adopted by the network (Siegelmann et al. 1997).

In NARX, each neuron in one layer was linked to each of the neurons in the next layer by means of a link along with connected weights. These weights were updated during the training cycles until the expected output was obtained. Neural network architecture includes three aspects: the information flow direction between neurons, the method to update the connection weight, and the transfer function which yields the output from the set of inputs made to the architecture (ASCE 2005).

Trials were conducted with different configuration parameters and these parameters were tested for their level of accuracy in forecasting snow covered area for different elevation zones.

The *LogSig* transfer function, Equation 4, was used in this study. The LogSig function scales the data between 0 and +1.

$$\log sig(p) = \frac{1}{(1+e^{-p})} \quad (4)$$

In general, NN models are able to approximate arbitrary complex linear and non-linear dynamical systems without making any assumptions about the underlying data and process. This simplifies the modeling (Sauter et al. 2009). In this study, we were interested in the pattern of snow covered rather than in the physical process itself. Therefore, the analysis of neural network (NN) was not so complex.

NARX is used to predict the snow cover percentage for the next month. The model estimated outcome from the network is used as feedback to input layer of the network and is subsequently used for the next calculation. As the recurrent networks are highly sensitive to small change (Cao and Wang 2004), there is a huge risk of over-fitting or under-fitting while training the network if the number of inputs or epochs is not appropriate. The training set is accepted as adequate if there is no big error in the accuracy indicators.

The selection of suitable input variables and their delays is a very critical factor while developing the model. For this study, the input variables were selected using the methodology indicated in section 3.1.

The gradient descent learning algorithm was selected for the calibration of the network. This algorithm attempts to find a point W in some parameter space such as the neural network weight space, which minimizes an error $e_i(m)$ and defined using the Equation 5:

$$e_i(m) = d_i(m) - y_i(m) \quad (5)$$

where $d_i(m)$ is from the system response at node i at iteration m, and the desired response $y_i(m)$ for a given input pattern.

The gradient descent algorithm starts at a random point in the weight space and moves downhill until a minimum in the error surface is found, moving in the direction of the steepest descent at each point. Each weight in the network can be adapted by error back propagation; i.e., the weight from node i to node j (w_{ij}) can be calculated by Equation 6:

$$w_{ij}(m+1) = w_{ij}(m) + \eta\delta_i(m)x_i(m) \quad (6)$$

where, x_i is a transform function at node i, and i and j indicate different layers.

The local error δ_i(m) can be directly computed from $e_i(m)$ at the output node or can be computed as a weighted sum of errors at the internal nodes. The constant η is learning rate.

3.3 Performance indicator

The accuracy of the simulated results was confirmed using two indicators: the Symmetric Mean Absolute Percentage Error (SMAPE) (Flores, 1986) and the Root Mean Square Error (RMSE). They are defined in Equations 7 and 8 (Jain et al. 2001; Babel and Shinde 2010).

$$SMAPE = \frac{1}{n}\sum_{I=1}^{n}\frac{|O_i - F_i|}{O_i + F_i} \times 100 \quad (7)$$

$$RMSE = \sqrt{\frac{1}{n}\sum_{i=1}^{N}(O_i - F_i)^2} \quad (8)$$

where O_i = observed snow cover; F_i = forecasted snow cover; and n = the total number of the testing datasets.

4 Results and Discussion

4.1 Input variables

Ten potential explanatory variables were identified, which were categorized under snow cover area, average temperature, minimum temperature, maximum temperature, precipitation, elevation, cloud cover days, frosty days, the wind speed and day of the year. But due to the unavailability of data, frosty days, wind speed and cloud cover days had to be discarded from consideration. For the remaining six parameters, the monthly data was collected from remote sensing sources such as MODIS, TRMM from January 2000 to December 2010. For these six parameters, the inter-correlation coefficient was obtained to each other. The summary of the correlation coefficients is given in Table 1. Elevation, minimum temperature and maximum temperature show a very good correlation

Table 1 Summary of the inter-correlation coefficient of selected input parameters

	Min temp	Max temp	Avg. temp	Precipitation	Elevation	Snow cover
Min temp	1.000	0.903	0.975	0.589	-0.897	-0.875
Max temp	0.903	1.000	0.976	0.549	-0.847	-0.840
Avg. temp	0.975	0.976	1.000	0.583	-0.894	-0.879
Precipitation	0.589	0.549	0.583	1.000	-0.342	-0.512
Elevation	-0.897	-0.847	-0.894	-0.342	1.000	0.787
Snow cover	-0.875	-0.840	-0.879	-0.512	0.787	1.000

coefficient with average temperature. Therefore, only average temperature was considered. Similarly, the precipitation and snow cover area in the previous months are not seeminlgy correlated to average temperature; thus, both of them were kept in consideration.

4.2 Training and testing

We used the meteorological time series data obtained from the input selection procedure mentioned in the section 3.1, as input variables to the NARX model in order to generate snow time series for snow cover.

A suitable training dataset was identified to train the model so that the model is not open to the risk of being overfit or underfit. The datasets between 2000 and 2007 were found to be optimum in order to train the model and the remaining dataset from January 2007 to December 2010 was used for testing. The testing set was also used as a reference period for changes in future scenarios.

While the network was being trained, the effect of each input on the network was also being studied. This provided feedback for the number of hidden layers and which transfer function was most suitable. Based on this feedback, it was decided to prune the input space by changing the number of hidden layers. That reduces the network's complexity and the time's complexity.

The input set included temperature (^{o}C), monthly accumulated precipitation and snow cover area in the previous month, which was incorporated into the NARX model with 4 hidden layers with the gradient descent learning function and the LogSig transfer function. As per the nature of the network, we could not exclude the previous month's snow cover area, and so we selected the input variables in section 4.1. Statistical tests and measurements tend to indicate that the NARX is able to produce snow cover area. In addition to that, we tested the effects of changing in temperature only and precipitation only in this study. All the tested models were presented in Table 2.

Table 2 Selected neural network models with different input combinations for selected climatic variability

Model	Input variables
A	Temperature, snow cover – previous month
B	Precipitation, snow cover – previous month
C	Temperature, precipitation and snow cover – previous month

Table 3 depicts the performance of a developed model with different combinations of input sets in all three elevation zones. These were evaluated using SMAPE and RMSE. The model was tested with three sets of input combination with the selected input variables, namely temperature with the snow cover area of the previous month as the feedback loop, precipitation with the snow cover area of the previous month as the feedback loop and temperature and precipitation along with the snow cover area of the previous month as the feedback loop. The RMSE is 2.16, 5.62 and 5.59 in zone II, zone III and zone IV, respectively. Similarly, the SMAP is 4.92, 4.72 and 2.56 in zone

Table 3 Performance indicators of tested NARX models for three elevation zones

Model	Zone II		Zone III		Zone IV	
	RMSE	SMAPE	RMSE	SMAPE	RMSE	SMAPE
A	7.67	19.6	11.67	12.9	12.35	8.85
B	7.38	29.02	13.09	20.62	9.58	5.49
C	2.16	4.92	5.62	4.72	5.59	2.56

Notes: RMSE =Root Mean Square Error; SMAPE= Symmetric Mean Absolute Percentage Error.

II, zone III and zone IV, respectively.

The zone III has the highest error among the three zones. This may be because of the very dynamic nature of snow cover of the zone. The temperature in this zone is always close to the melting/freezing temperature. The majority of the precipitation is in the form of snow and immediately melt-up thus the snow cover is changing very rapidly and very difficult to capture the real situation from satellite images.

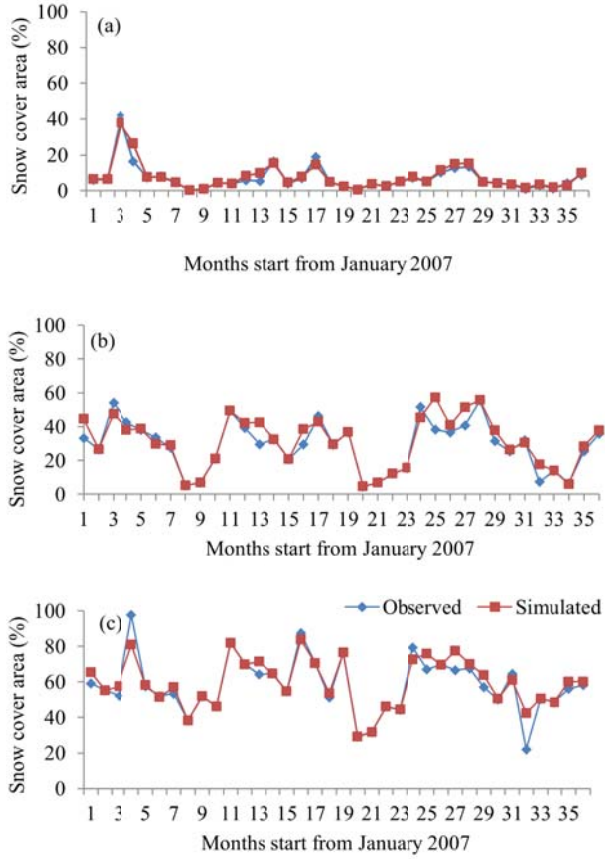

Figure 3 Snow cover area simulated vs. observed. (a) zone II, (b) zone III and (c) zone IV using nonlinear autoregressive exogenous model LogSig 4 hidden layers.

Figure 3 demonstrates the time series simulated snow cover in comparison to the observed snow cover in all three zones for the best performing model C (temperature, precipitation and snow cover in the previous month are input set). In order to test the temporal effect on the predicted snow cover area, the Sen's slope was computed from the error (observed snow cover area (%) - predicted snow cover area (%)). From the test, it is found that, the error is increased by -0.017%, 0.030%, and 0.055% per month in zone II, zone III and zone IV, respectively. For example, the error in the n^{th} month is increased by 0.055% than that in the $(n-1)^{th}$ month in zone IV. Surprisingly, the error in zone II is decreased as the lead-time increased, that is because of a very big overestimation in the second and third month, if we ignore these outlier values, then the error increasing rate will become 0.024. Therefore, all these error increasing rates implied that the model's performance decreased as the lead time increased. However, it is very small.

This is because of the uses of forecasting snow cover. This finding is similar to earlier work by Hung et al. (2009). Even though the performance is decreasing as the time increases, the rate of decrease is not so high; therefore, we believe this model can be used for long term snow cover forecasting. The performance of forecasting depends mainly on input parameters such as temperature, precipitation and snow cover in the previous month. Since the accuracy of the simulated snow cover area is decreasing with the increasing in lead time, so as in every further forecasting, the error will accumulate, on this account, as the lead time increases, the performance may decrease gradually.

4.3 Predicting future snow cover

The selected neural network model C was used to simulate snow cover area in the Kaligandaki basin in the three upper zones (Zone II, Zone III, and Zone IV) separately for the next thirty years. The HadCM3 A1B scenario was considered for the simulation. Temperature and precipitation were downscaled to a 0.25° resolution for the input. Figure 4 illustrates the snow cover scenario in Zone II, Zone III and Zone IV from January 2011 to December 2040, in accordance with the HadCM3 A1B scenario.

From the graph, we can see that the glacier area will significantly decrease in the Kaligandaki basin. In Zone III, there will be a substantial area covered by snow in winter and pre-spring. Otherwise, it will be completely free from snow. With respect to Zone II, very little and sporadic snow will be seen in autumn, winter and spring seasons

Figure 5 shows the changes in snow cover area in all the three zones in the 2000-2010 average

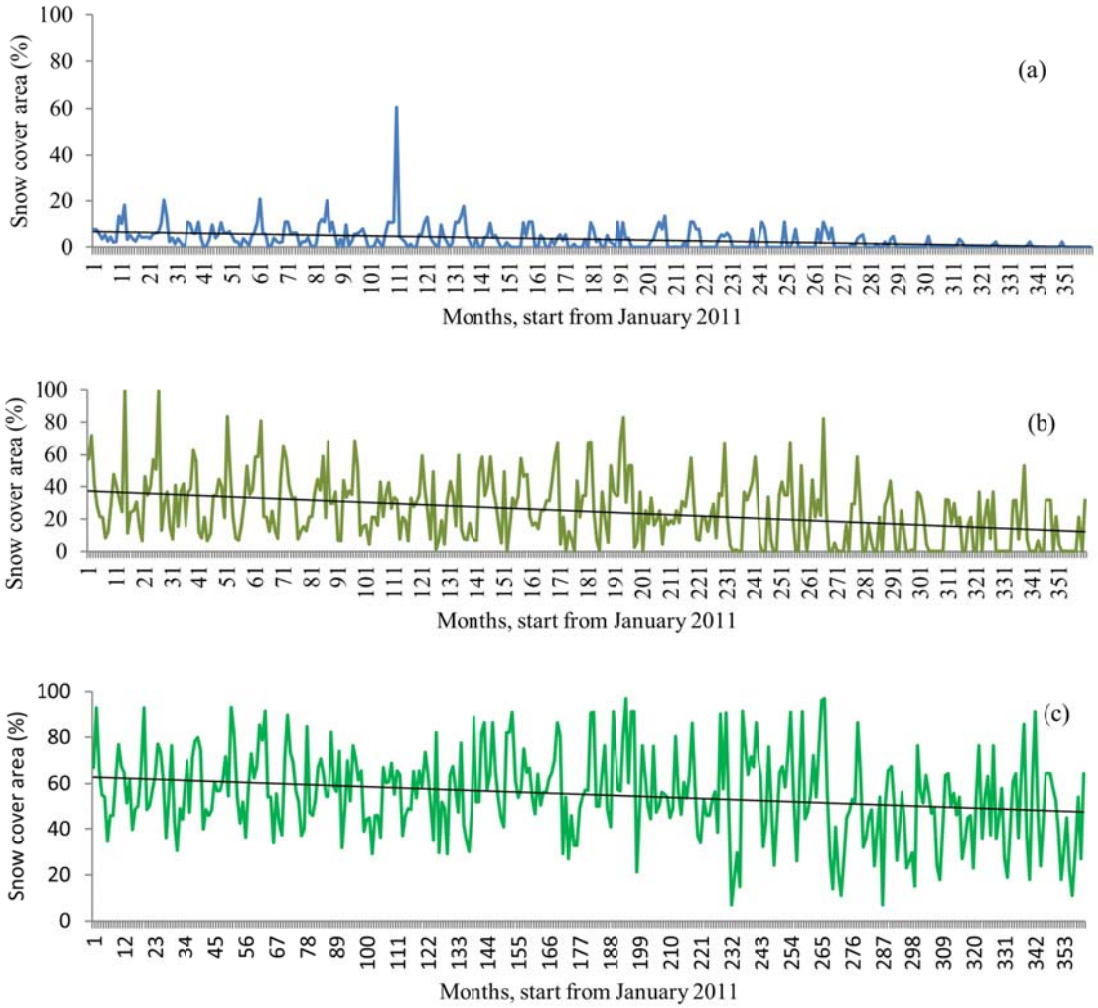

Figure 4 Time series snow cover extent forecasting using nonlinear autoregressive exogenous model and HadCM3 A1B scenario 2011 to 2040 (a) zone II, (b) zone III, and (c) zone IV with precipitation and temperature are exogenous input.

snow cover and 2030-2040 average snow cover. The blue dots represent the mean snow cover area (%) computed from MODIS during 2000-2010 and the red dots represents the mean snow cover area (%) obtained from the simulation. The absolute changes are indicated by rectangles (decrease) and blank rectangles (increase).

The 10% prediction bounds (black line) for each month are shown in Figure 5. If the changes are greater than the derived prediction bounds, the changes in snow are significant. According to the model's output, we may expect that the snow cover extent will start to shrink due to the increase in temperature or decrease in precipitation.

With regards to Zone IV and higher elevations, snow cover seems more persistence. However, the thickness of the snow deposit may decrease significantly in the future; therefore, the study of snow thickness in this zone is promising. Changes are not significant in Zone IV in comparison to Zone III. Zone II already has very low snow cover area; therefore, the snow cover changes do not seem significant. However, in several months of the year, this area will be completely snow free.

The major exogenous input for the model are temperature and precipitation, thus, if the temperature goes down and the precipitation occurs at the same time it is likely to have a snowfall. Therefore, having shown some snow in winter in zone I would not be an extreme situation, however, if the snow cover is persistent for several weeks to months and the snow cover area is significantly higher at least come to the considerable figure then the situation should

consider as an extreme situation.

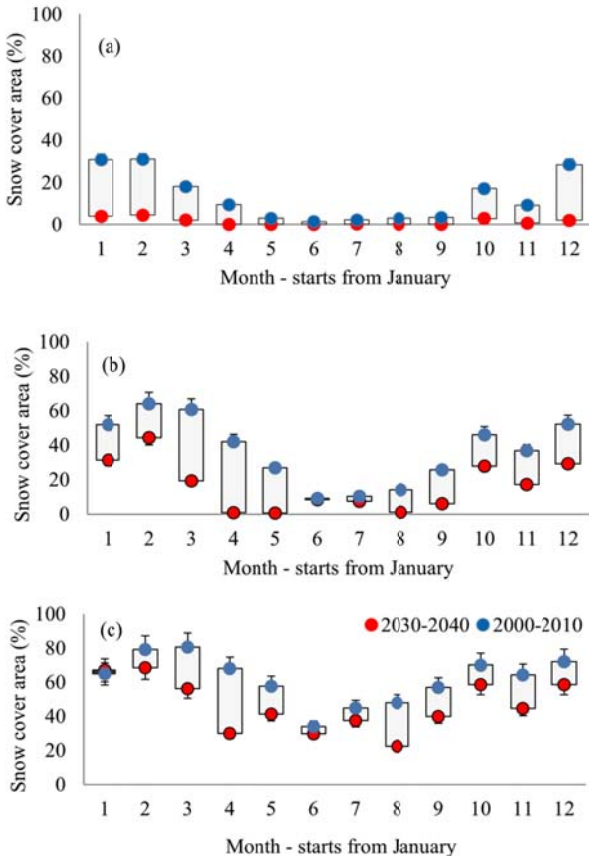

Figure 5 Monthly snow cover extends changes over 2000-2010 vs. 2030-2040, (a) zone II, (b) zone III, and (c) zone IV. The blue bubbles represent the snow cover area in 2000-2010 and the red bubbles represent the snow cover area in 2030-2040, and the square represents the changes in average snow cover of 2000-2010 to that of 2030-2040.

The snow cover area is not only the function of the temperature and precipitation of a corresponding season, but also the snow accumulation during previous seasons or months. As some decrements of the snow cover area can be observed in winter, due to increasing temperature and decreasing precipitation trends in a spring substantial decrease in snow cover area may be observed. As far as autumn is concerned, it should be noted that the temperature and precipitation trends not only impact the snow cover area, but also snow depth/snow accumulation is very important for the persistent snow cover in the summer. Due to the less accumulation in the winter, most of the snow may melt up until the end of late summer and may result in significant decrement in the snow cover area in autumn.

The decreasing snow cover area has multi-dimensional effects on the socio-economic condition of the local people. The life of the local people expects to be easier than before due to the favorable weather condition. Growing of the vegetation in the higher altitude makes possible for cultivation and growing vegetables. The major profession of the people in this basin is tourism and apple farming, due to the less chilly environment the tourism industry is likely to grow, however, apple farming will destroy and effects are already visible. Due to the warmer environment the produced apple are not as delicious as before (Dahal et al. 2009) and emergent of sever types of insects is also a big threat for apple farming. In addition to this, the threat of vector borne disease also increased in the higher altitudes (Mishra et al. 2013). Thus, a socio economic reform can happen. On the other hand, due to the shrinking snow cover area, the flow in the Kaligandaki River will likely to decrease in spring, summer and autumn and may threat the livelihood of more than one million people in the downstream area.

5 Conclusions

An approach to predict the snow cover area using NARX, an ANN model, has been presented in this paper. The model is based on meteorological data obtained from the global climate simulation based on A1B scenario. The ten years' snow extent was generated from a MODIS product for the Kaligandaki basin for the period of 2000-2010. This data was used for training and testing the model. The time series snow cover percentage in each zone was forecasted using the NARX for 2011-2040.The snow cover prediction is intended for the study of water availability in this basin where approximately 300 thousand people are directly dependent on the water from this river. Depending on the scenario selected, the model demonstrated a decrease in snow cover based on the elevation zones. Zone III shows the maximum influence under the climate change scenario and Zone IV the minimum. However, the decrease in snow cover in Zone IV is also significant and the study of snow thickness in this zone is important to understand the ever-changing phenomenon of climate.

The simulated results demonstrate that climate change will have an adverse effect on the

snow cover area in the study area under consideration. This is possibly the first study in this region to forecast snow cover with this resolution. The results are somewhat expected and are generally consistent, even without an understanding of the snow process. The magnitude of the reduction in snow cover is higher in the transition area i.e. the maximum effect can be seen in Zone III.

While the results presented are consistent and reasonable in our understanding, we must still exercise some caution in their use. Foremost is the warning that this forecasting is based on GCM data, in which uncertainty is inherent. Additionally, the developed model could have some bias and may give rise to some anomalies. Furthermore, we have used remote sensing data that also inherits several uncertainties. In addition, we did not have data regarding snow depth in our study. Snow depth is a vital factor, so we recommend considering snow depth as well in order to forecast the consistency of the snow cover area. Therefore, future work may consider these and other related issues through the coupling of a regional climate model by exploring an optional advanced ANN to better simulate future climate scenarios and can study the potential impacts of these scenarios on water availability in the Kaligandaki basin.

Acknowledgements

The authors would like to thank the Asian Institute of Technology (AIT) for providing the platform for this research. They would also like to express their sincere gratitude to the Government of Japan for providing a scholarship to the first author of the paper.

References

ASCE Task Committee on Application of Artificial Neural Networks in Hydrology (2005) Artificial neural networks in hydrology: preliminary concepts. Journal of Hydrologic Engineering 5: 115-123.

Babel MS, Shinde VR (2010) Identifying prominent explanatory variables for water demand prediction using artificial neural networks: A case study of Bangkok. Water Resources Management 25: 1653-1676. DOI: 10.1007/s11269-010-9766-x.

Besaw LE, Rizzo DM, Bierman PR, et al. (2010) Advances in ungauged stream flow prediction using artificial neural networks. Journal of Hydrology. 386: 27-37. DOI: 10.1016/ j.jhydrol.2010.02.037.

Bolch T, Kulkarni A, Kääb A, et al. (2012) The state and fate of Himalayan Glaciers. Science 336: 310-314. DOI: 10.1126/ science.1215828.

Cao J, Wang J, (2004) Absolute exponential stability of recurrent neural networks with Lipschitz-continuous activation functions and time delays. Neural Networks 17: 379-390. DOI: 10.1016/j.neunet.2003.08.007.

Chatterjee A, Adak A, Singh AK, et al. (2010) Aerosol chemistry over a high altitude station at Northeastern Himalayas, India. PLoS ONE 5(6): e11122. DOI: 10.1371/journal.pone.0011122.

Chen C, Chen BP, Chou FN, et al. (2010) Development and application of a decision group back propagation neural network for flood forecasting. Journal of Hydrology 385: 173-182. DOI: 10.1016/j.jhydrol.2010.02.019

Chen Y and Chang F (2009) Evolutionary artificial neural networks for hydrological systems forecasting. Journal of Hydrology 367: 125-137. DOI:10.1016/j.jhydrol.2009.01.009.

Connor JT, Martin RD, Atlas LE (1994) Recurrent neural networks and robust time series prediction. IEEE Transactions on Neural Networks 5(2): 240-254. DOI: 1045-9227/94.

Cooke K. (2014) Himalaya Glacial Melt Set to Peak by 2080. Available online: http://www.rtcc.org/2013/08/12/himalaya-glacial-melt-set-to-peak-by-2070/ (Accessed on 10 March 2014).

Dahal N, Ojha H, et al. (2009) Impact of climate change on forests livelihoods: issues and options for Nepal, Livelihoods and Forestry Programme, 17-25.Dery SJ, Salomonson VV, Stieglitz M, et al. (2005) Ann approach to using snow areal depletion curves inferred from MODIS and its application to land surface modelling in Alaska. Hydrological Process 19: 2755-2774. DOI: 10.1002/hyp.5784.

Decesari S, Facchini MC, Carbone C, et al. (2010) Chemical composition of PM10 and PM1 at the high-altitude Himalayan station Nepal Climate Observatory-Pyramid (NCO-P) (5079 m a.s.l.). Atmospheric Chemistry and Physics 10: 4583-4596. DOI: 10.5194/acp-10-4583-2010.

Diaconescu E (2008) The use of NARX neural networks to predict chaotic time series. Wseas Transactions on Computer Research 3(3): 182-191.

Flores BE (1986) A pragmatic view of accuracy measurement in forecasting. Omega14(2): 93-98. DOI: 10.1016/0305-0483(86)90013-7

Hall DK, Riggs GA, Salomonson VV (1995) Development of methods for mapping global snow cover using moderate resolution image spectro-radiometer data. Remote Sensing of Environment 54(6): 127-140. DOI: 10.1016/0034-4257(95) 00137-P

Hall D K, Salomonson VV, Riggs. GA (2006) MODIS/Terra Snow Cover 8-Day L3 Global 500 m Grid.Version 5. [indicate subset used]. National Snow and Ice Data Center, Boulder, Colorado, USA.

Hantel M, Hirtl-Wielke LM (2007) Sensitivity of Alpine snow cover to European temperature. International Journal of Climatology 20: 615-640. DOI: 10.1002/joc.1472.

Hendrikx J, Hreinsoon EO (2012) The potential impact of climate change on seasonal snow in New Zealand: part II-industry vulnerability and future snow making potential. Theoretical and Applied Climatology 110:619-630. DOI: 10.1007/s00704-012-0713-z.

Huffman GJ, Adler RF, Bolvin DT, et al. (2007) The TRMM multisatellite precipitation analysis (TMP): Quasi-global, multiyear, combined sensor precipitation estimates at fine scales. Journal of Hydrometeorology 8: 38-55. DOI: 10.1175/ JHM560.1.

Hung, NQ, Babel, MS, Weeskul, S, et al. (2009) An artificial neural network model for forecasting in bangkok, Thiland. Hydrology and Earth System Science 13: 1413-1425. DOI: 10.5194/hess-13-1413-2009.

IPCC (2007) Climate change 2007: Impacts, Adaptation and Vulnerability. Cambridge University Press, Cambridge, UK.

Jain A, Varshney AK, Joshi UC (2001) Short term water demand forecast modelling at IIT Kanpur using artificial neural networks. Water Resources Management 22(6): 299-321. DOI:10.1023/A:1014415503476.

Karmacharya J, Shrestha A, Shrestha ML (2007) Climate change scenarios for South Asia and Central Himalayan region Based on GCM Ensemble. Department of Hydrology and Meteorology Kathmandu, Nepal.

Khadka D, Babel MS, Shrestha S and Tripathi NK (2014) Climate change impact on glacier and snow melt and runoff in Tamakoshi basin in the Hindu Kush Himalayan (HKH) region, Jornal of Hydrology 511:49-60, DOI: http://dx.doi.org/10.1016/j.jhydrol.2014.01.005.

Klein AG, Hall DK., Riggs GA (1998) Improving snow-cover mapping in forests through the use of a canopy reflectance model. Hydrological Processes 12:1723-1744. DOI: 10.1002/(SICI)1099-1085(199808/09)12:10/11<1723::AID-HYP691>3.0.CO;2-2.

Kulkarni AV, Bahuguna IM, Rathore BP, et al. (2007) Glacial retreat in Himalaya using Indian remote sensing satellite data. Current Science 92(1): 69-74. DOI: 10.1117/12.694004.

Li Z, Xing Q, Liu S, et al. (2012) Monitoring thickness and volume changes of the Dongkemadi Ice Field on the Qinghai-Tibetan Plateau (1969-2000) using Shuttle Radar Topography Mission and map data. International Journal of Digital Earth 5(6): 516-532 DOI: 10.1080/17538947.2011.594099.

Maier HR, Jain A, Dandy GC, et al. (2010) Methods used for the development of neural networks for prediction of water resource variables in river systems: Current status and future directions, Environmental Modelling and Software 25: 891–909. DOI: 10.1016/j.envsoft.2010.02.003.

Mallapaty S, (2014) Himalayan Glaciers Debate: Melting or Growing. Available online: http://www.scidev.net/global/climate-change/feature/himalayan-glaciers-debate-melting-or-growing--1.html. (Accessed on 10 March 2014).

Maskey S, Uhlenbrook S, Ojha S (2011) An analysis of snow cover changes in the Himalayan region using MODIS snow products and in-situ temperature data. Climate Change 108: 391-400. DOI: 10.1007/s10584-011-0181-y.

Mishra B, Babel MS, Tripathi NK (2014) Analysis of climatic variability and snow cover in the Kaligandaki River Basin, Himalaya, Nepal. Theoretical and Applied Climatology 116: 681-694. DOI: 10.1007/s00704-013-0966-1.

Mishra B, Ghimire BR, Baral D, et al. (2013), Japanese Encephalitis risk zone mapping using remote sensing data: a case study of Mid and Far-Western part of Nepal. Journal of Remote Sensing 4: 47-55.

Noori R, Sabahi MS, Karbassi AR, et al. (2010) Multivariate statistical analysis of surface water quality based on correlationsand variations in the data set. Desalination 260: 129-136. DOI: 10.1016/j.desal.2010.04.053.

Nourani V, Hosseini BA, Daneshvar VF, et al. (2012) Classification of groundwater level data using SOM to develop ANN-based forecasting model. International Journal of Soft Computing and Engineering 2(1): 464-469.

Pope VD, Gallani ML, Rowntree PR, et al. (2000) The impact of new physical parameterizations in the Hadley Centre climate model – HadAM3. Climate Dynamics 16(2-3): 123-146. DOI: 10.1007/s003820050009

Quiroga VM, Mano A, Asaoka Y, et al. (2013), Snow glacier melt estimation in tropical and an glaciers using artificial neutral network. Hydrology and Earth System Sciences 17: 1265-1280. DOI: 10.5194/hessd-9-9455-2012.

Rees HG, Collins DN (2006) Regional differences in response of flow in glacierfid Himalayan rivers to climatic warming. Hydrological Process 20: 2157-2169. DOI: 10.1002/hyp.6209.

Riggs GA, Hall DK, Salomonson VV (2006) MODIS snow products user guide to collection 5. NSID C1–80.

Sauter T, Schneider C, Kilian R, et al. (2009) Simulation and analysis of Runoff from a partly glaciated meso-scale catchment area in Patagonia using an artificial neural network. Hydrological Processes 23: 1019-1030. DOI: 10.1002/hyp.7210.

Sauter T, Weitzenkamp B, Schneider C (2010) Spatio-temporal prediction of snow cover in the black forest mountain range using remote sensing and a recurrent neural network. International Journal of Climatology 30: 2330-2341. DOI: 10.1002/joc.2043.

Kronenberg R, Barfus K, Franke J, et al. (2013) On the downscaling of meteorological fields using recurrent networks for modelling the water balance in a meso-scale catchment area of Saxony, Germany. Atmospheric and Climate Sciences 3(4): 552-561. DOI: 10.4236/acs.2013.34058 P

Shen HY, Chang LC (2013) Online multistep-ahead inundation depth forecasts by recurrent NARX networks. Hydrology and Earth System Sciences 17: 935-945. DOI: 10.5194/hess-17-935-2013.

Stres B, Philippot L, Faganeli J, et al. (2010) Frequent freeze-thaw cycles yield diminished yet resistant and responsive microbial communities in two temperate soils: a laboratory experiment. FEMS Microbiology Ecology 74(2): 323-35. DOI: 10.1111/j.1574-6941.2010.00951.x.

Stres B, Sul WJ, Murovec B, et al. (2013) Recently deglaciated high-altitude Soils of the Himalaya: diverse environments, heterogenous bacterial communities and long-range dust inputs from the upper troposphere. PLoS ONE 8(9): e76440. DOI: 10.1371/journal.pone.0076440

Siegelmann HT, Horne BG, Giles CL (1997) Computational capabilities of recurrent NARX neural networks. IEEE Transactions on Systems, Man, and Cybernetics 27(2): 208-215. DOI: 10.1109/3477.558801

Welsh W (2008) Water balance modeling in brown, Queensland, and the ten iterative steps in model development and evaluation. Environmental Modelling and Software 23: 195-205. DOI: 10.1016/j.envsoft.2007.05.014

Wang K, Wan Z, Wang P, et al. (2007) Evaluation and improvement of the MODIS land surface temperature/emissivity products using ground-based measurements at a semi-desert site on the western Tibetan Plateau. International Journal of Remote Sensing 28: 2549-2565. DOI: 10.1080/01431160600702665

Wang W, Liang S, Meyers T (2008) Validating MODIS land surface temperature products using long-term night time ground measurements. Remote Sensing of Environment 112: 623-635. DOI:10.1016/j.rse.2007.05.024

Xu J, Grumbine RE, Shrestha A, et al. (2009) The melting Himalayas: cascading effects of climate change on water, biodiversity, and livelihoods. Conservation Biology 23(3): 520-530. DOI: 10.1111/j.1523-1739.2009.01237.x